MJFAS
Malaysian Journal of Fundamental and Applied Sciences

Lestari *et al.* | Malaysian Journal of Fundamental and Applied Sciences, Vol. 21 (2025) 2905–2914

RESEARCH ARTICLE

Lung Cancer Classification Based on a Small Dataset of X-Ray Images Using Transfer Learning Deep Boltzmann Machine

Fauzia P. Lestari*, Freddy Haryanto, Sparisoma Viridi, Mohammad Haekal, Idam Arif

Department of Physics, Faculty of Mathematics and Natural Sciences; Institut Teknologi Bandung, Jl. Ganesha 10, Bandung, Indonesia, 40132

Abstract Deep learning has shown significant potential in medical image classification; however, its effectiveness is often limited by the need for large, labeled datasets. In the context of lung cancer detection via X-ray images, the scarcity of annotated data poses a major challenge. This study introduces a Transfer Learning approach integrated with Deep Boltzmann Machines (TL-DBM) to address this limitation. Publicly available datasets such as MNIST and CIFAR-10 were leveraged to pre-train the DBM model, extracting transferable parameters for further training on chest X-ray images. The statistical correlation between source and target images and mean-field inference iterations during training assessed and adjusted to improve performance. Our experiments reveal that using CIFAR-10 source data—specifically airplane and dog categories—and applying a 10-step mean-field process yields the highest classification accuracy of 89.4%, compared to 65.4% without transfer learning. These findings suggest that TL-DBM offers an effective strategy for lung cancer image classification in data-constrained settings.

Keywords: Classification, DBM, Transfer Learning, Lung Cancer, X-ray.

Introduction

Lung cancer is the second-deadliest disease in the world based on GLOBOCAN data (Sung et al., 2021; Jensen et al., 2002). Cancer patients are often treated late due to delayed diagnosis (Deng, 2012; Jensen et al., 2002). To perform a diagnosis, doctors perform screening using a CT scan or traditional Chest X-ray (CXR). The CT-Scan and CXR images must then be read by a competent doctor to get a precise diagnosis. However, the limitations of the number of experienced doctors led to a slow diagnosis because there is too much data to read compared to the number of doctors. There is a need for a method that can help speed up the classification process of these images.

Today artificial intelligence is highly developed and used in many fields. In classical supervised machine learning, using a shallow layer, the more labeled data, the better the result (Najafabadi et al., 2015; Willemink et al., 2020). Whereas in deep learning, by utilizing many layers of nonlinear processing, we can use a few labeled data models can achieve good performance with few labeled data when supported by approaches such as transfer learning (Pan & Yang, 2010; Raghu et al., 2019; Willemink et al., 2020). This is particularly relevant in medical imaging, where annotated datasets are often scarce. Deep Boltzmann Machine (DBM) is a deep learning method developed from the Restricted Boltzmann Machine (Hinton et al., 2006). (Bengio et al., 2007) method. DBMs are particularly well-suited for transfer learning because they learn deep hierarchical generative representations that can be transferred from large source datasets to smaller domain-specific datasets (Bengio, 2009; Salakhutdinov & Larochelle, 2010; Srivastava & Salakhutdinov, 2012). DBM requires pre-training procedures to make DBM training more efficient. DBM can be used for training unlabeled data and can be used for fine-tuned using little labeled data (Hinton et al., 2006; Salakhutdinov & Larochelle, 2010).

***For correspondence:**
fauzia@itb.ac.id

Received: 17 June 2025
Accepted: 3 Sept. 2025

However, the amount of data required for training on deep learning models is huge often very large (Eertink et al., 2022; Najafabadi et al., 2015). Meanwhile, the amount of CXR data for lung cancer cases is so limited that it becomes a challenge to use deep learning. Transfer Learning is a learning method to gain knowledge from other data training to complete the target data training task (Torrey & Shavlik, 2010). Recent studies have highlighted that transfer learning significantly improves performance in medical imaging tasks with limited data, including radiology and chest X-rays (Ait Nasser et al., 2023; Raghu et al., 2019; Ranzato et al., 2010). These works strengthen the motivation for adapting transfer learning within DBMs to address lung cancer classification using small datasets. Transfer learning can speed up the training process,. Transfer learning while also allows for deep learning to be used with few target data, since it previously used pretraining result parameter data from source data (Litjens et al., 2017; Torrey & Shavlik, 2010).

In this study, we propose a transfer learning deep Boltzmann machine (TL-DBM) method. This method utilizes DBM pretraining results with a large number of source image datasets, and the parameters of the DBM pretraining results are used for training CXR data with a limited amount of data. Pretraining DBM is a layer-by-layer greedy consisting of a stack of Restricted Boltzmann Machines (RBMs) with few modifications. To estimate data-dependent expectations, mean-field interference is used in pretraining procedures. Furthermore, to determine the source data label that provides maximum results with the target data, we evaluate the correlation between the source image and the target image.

Materials and Methods

The Deep Boltzmann Machine used in this paper has three hidden layers (L=3), consisting of 500 units in the first layer (h^1), 500 units in the second layer (h^2), and 2000 units in the third layer (h^3). These numbers were selected based on prior DBM literature (Salakhutdinov & Larochelle, 2010; Srivastava & Salakhutdinov, 2012) and our preliminary experiments, to balance model capacity with the risk of overfitting when working with a small dataset (Bengio, 2009). with the energy of state $\boldsymbol{v}$, $\boldsymbol{h}$ defined

$$E(\boldsymbol{v},\boldsymbol{h};\theta) = -\boldsymbol{v}^T\boldsymbol{W}^1\boldsymbol{h}^1 - \boldsymbol{h}^{1T}\boldsymbol{W}^2\boldsymbol{h}^2 - \boldsymbol{h}^{2T}\boldsymbol{w}^3\boldsymbol{h}^3 \tag{1}$$

Where $h = h^1, h^2, h^3$ are the hidden units, and $\theta = \{W^1, W^2, W^3\}$ are the model parameters. The probability of the model is

$$P(v;\theta) = \frac{P^*(v;\theta)}{Z(\theta)} = \frac{1}{Z(\theta)}\sum_h \exp(-E(\boldsymbol{v},\boldsymbol{h}^1,\boldsymbol{h}^2,\boldsymbol{h}^3;\theta)) \tag{2}$$

$$\log P(v;\theta) \geq v^T W^1\mu^1 - \mu^{1T}W^2\mu^{2-\mu^{2T}}W^3\mu^3 - \log Z(\theta) + \mathcal{H}(Q) \tag{3}$$

$\mathcal{H}(Q)$ is the entropy function with $\mu = \mu^1, \mu^2, \mu^3$ are the mean field parameters with

$$\mu_j^1 \longleftarrow \sigma\left(\sum_{i=1}^{D} W_{ij}^1 v_i + \sum_{k=1}^{F_2} W_{jk}^2\mu_k^2\right) \tag{4}$$

$$\mu_k^2 \longleftarrow \sigma\left(\sum_{j=1}^{F_2} W_{jk}^2\mu_j^1 + \sum_{m=1}^{F_3} W_{km}^3\mu_m^2\right) \tag{5}$$

$$\mu_m^3 \longleftarrow \sigma\left(\sum_{k=1}^{F_2} W_{km}^3\mu_m^2\right) \tag{6}$$

The proposed TL-DBM framework consists of three stacked RBM layers used for greedy pretraining on the source dataset, followed by a Deep Boltzmann Machine (DBM) that integrates the pretrained parameters and is fine-tuned with the target dataset. In this architecture, the DBM serves as the final classification stage after transfer of knowledge from the source data. The proposed method differs from conventional transfer learning approaches (e.g., pretrained CNN followed by fine-tuning) in three main aspects. First, we employ Transfer Learning on a Deep Boltzmann Machine (TL-DBM),

where the DBM acts as the main feature extractor after a pretraining stage on the source dataset (MNIST or CIFAR-10). The pretrained parameters are then transferred and fine-tuned with the target dataset (JSRT). Second, instead of arbitrarily selecting source data, we compute the statistical correlation between source and target images to identify the most relevant source classes for transfer. Third, during fine-tuning, we vary the number of mean-field iterations in order to examine the trade-off between classification accuracy and computational cost. These design choices differentiate TL-DBM from conventional CNN-based transfer learning pipelines and are summarized in Figure 1: Figure 1 shows the outline proposed method and the algorithm is described below

(1) Pre-processing images made the format and size uniform.
(2) Evaluate the greedy pretraining DBM to get weights using the source data
(3) Evaluate the correlation between the source and target image to choose the best suitable labelled the source images
(4) Process the DBM algorithm with mean field interferences using Eq (4), (5), and (6) using the previous parameters but using target data (Hinton et al., 2006; Salakhutdinov & Larochelle, 2010).

For the greedy pretraining Boltzmann machine, we used 3 RBMs to train source data. We evaluated MNIST (Bengio, 2009; Deng, 2012) and cifar10 (Ait Nasser et al., 2023; Krizhevsky et al., n.d.) dataset for the source data. MNIST dataset has 60000 28x28 pixels grayscale number handwriting images with 10 categories for training dataset and 10000 images for test dataset. Cifar10 has 32x32 pixels 50000 of various colour images of 10 categories for training and 10000 images for test dataset. The 10 categories are airplane, automobile, bird, cat, deer, dog, frog, horse, ship, truck. The target data we used Japanese Society of Radiological Technology (JSRT) (Hussain et al., 2020; Shiraishi et al., 2000). JSRT consists of 154 conventional chest radiographs with 154 lung nodule and 93 images without nodule. We divided JSRT dataset into 70% data training and 30% data test randomly. To ensure robustness, this random split was repeated five times with different seeds, and the reported accuracy is the average across all trials. This approach aligns with recommendations for small sample sizes, where single hold-out splits suffer from large uncertainty, and repeated validation is preferred (Eertink et al., 2022).

To evaluate correlation between source (X) and target images (Y), we used following equation

$$\frac{\sum_m \sum_n (X_{mn} - \bar{X})(Y_{mn} - \bar{Y})}{\sqrt{(\sum_m \sum_n (YX_{mn} - \bar{Y}\bar{X})^2)(\sum_m \sum_n (Y_{mn} - \bar{X}\bar{Y})^2)}} \quad (7)$$

In DBM process, we updated the mean-field interferences. We did several experiments about the number of mean-field iterations. Fine tuning was also done for the target data parameters.

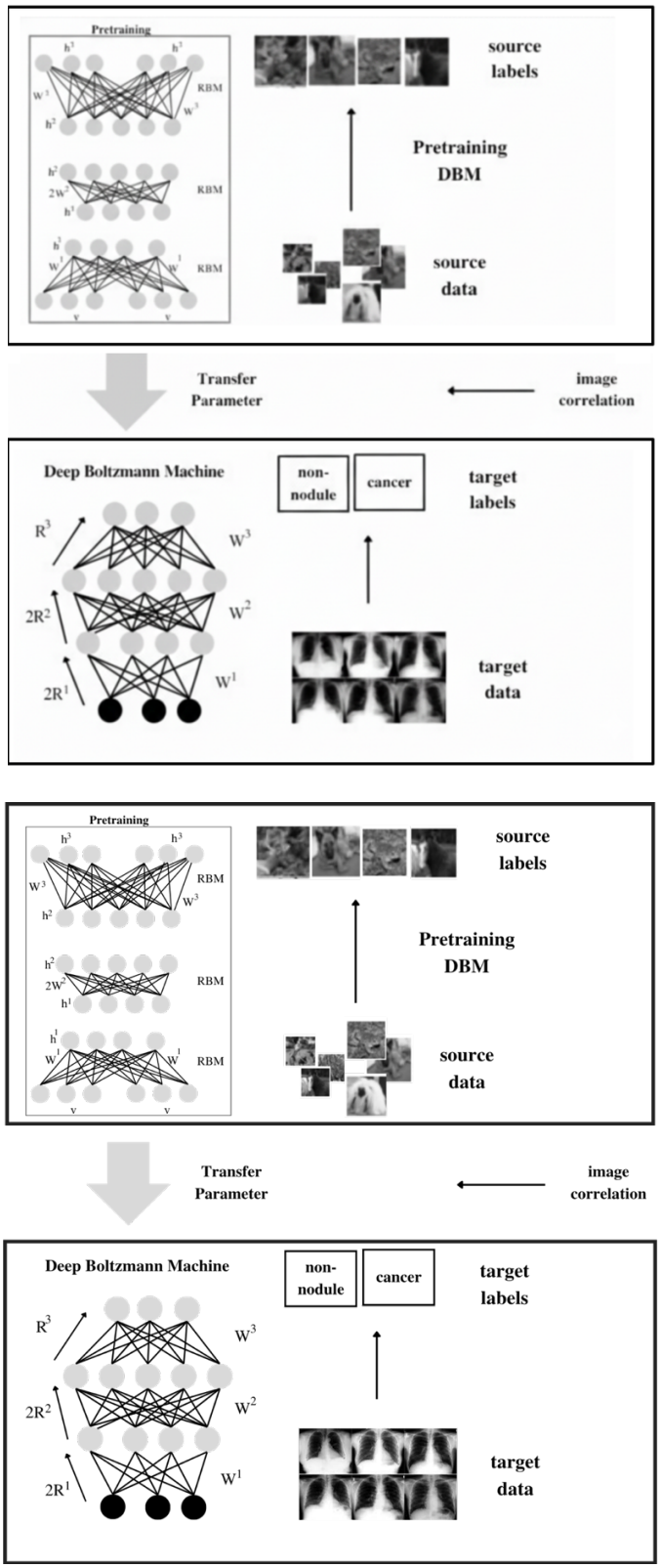

Figure 1. Outline for the proposed method TL-DBM framework. Unlike conventional transfer learning (e.g., CNN fine-tuning), our method uses DBM as the main feature extractor after RBM pretraining, incorporates correlation-based source dataset selection, and explores mean-field iteration tuning to balance accuracy and efficiency

Results and Discussion

For pre-processing, we made all data uniform. For the MNIST experiment, we made JSRT images to 28x28 pixels. For the Cifar10 experiment, JSRT images are resized to 32x32 pixels. Both for MNIST and cifar10, datasets were calculated in batch of 100. Because cifar10 has 3 layers red, green, blue layers, we made JSRT pixel value in three layers identically for red, green, and blue layers. We divided JSRT dataset into 70% data training and 30% data test randomly. Figure 2 shows the example of the dataset.

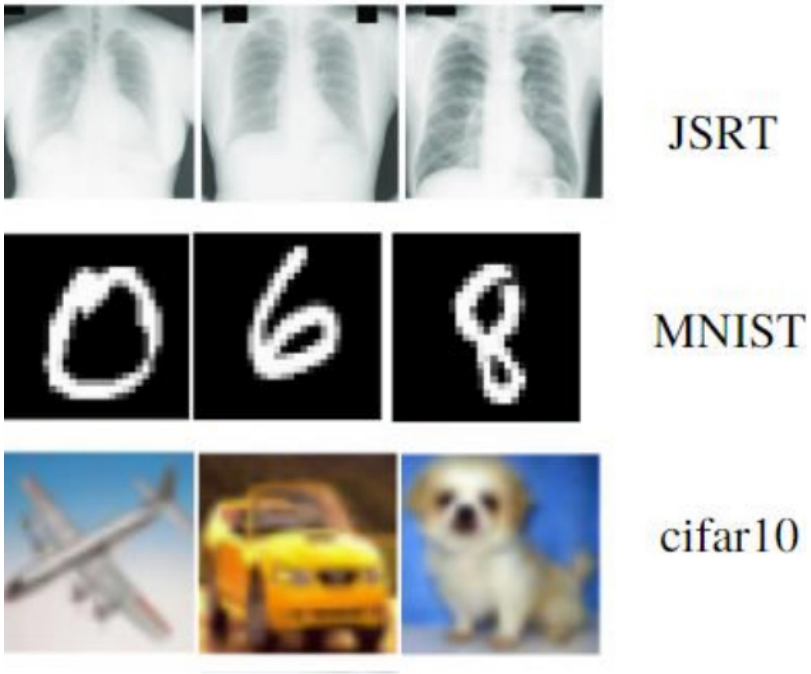

Figure 2. Example of datasets

Figure 3 Shows the results for the correlation between MNIST and JSRT dataset. On average, correlation between non-nodule with MNIST dataset is 0.0951 and 0.0665 for the cancer dataset. The maximum correlation both non-nodule and cancer images are with digit “0”. We could not use the same label for the training, so we tried to evaluate performance of the proposed method by using two cases (digit “0” as non-nodule, digit “8” as cancer) and (digit “5” as non-nodule and digit “0” as cancer data).

Figure 3 shows that correlations between MNIST digits and JSRT images are generally weak (≤ 0.1). This indicates that structural similarity between handwritten digits and lung radiographs is limited, which explains why transfer from MNIST produced only modest improvements in performance (see Table 1).

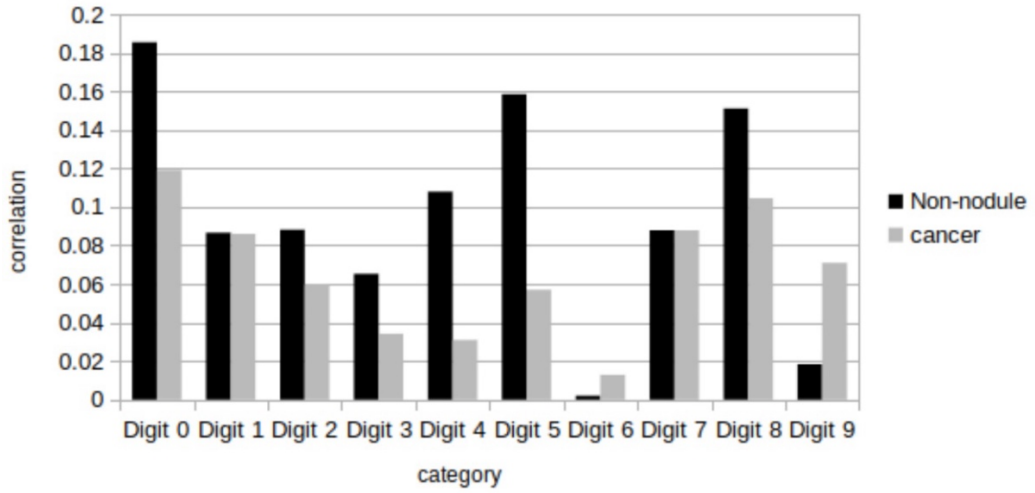

Figure 3. Correlation between MNIST and JSRT dataset

Figure 4 Shows the results for the correlation between cifar10 and JSRT dataset. On average, correlation between cifar10 and JSRT is better than MNIST and JSRT dataset, which is 10.1851 for non-nodule and 10.165 for the cancer dataset. The maximum correlation for non-nodule is 0.325 with category-1 (airplane) and for cancer is 0.245 with category-6 (dog). One plausible explanation is that airplane images often contain large homogeneous regions with sharp edge contrasts, while dog images exhibit fine-grained textures and high-frequency patterns. These characteristics more closely resemble the structural and textural properties of lung X-rays—such as alveolar patterns, vascular markings, and boundary delineations—compared to categories like ship or truck (Ranzato et al., 2010; Ait Nasser et al., 2023).

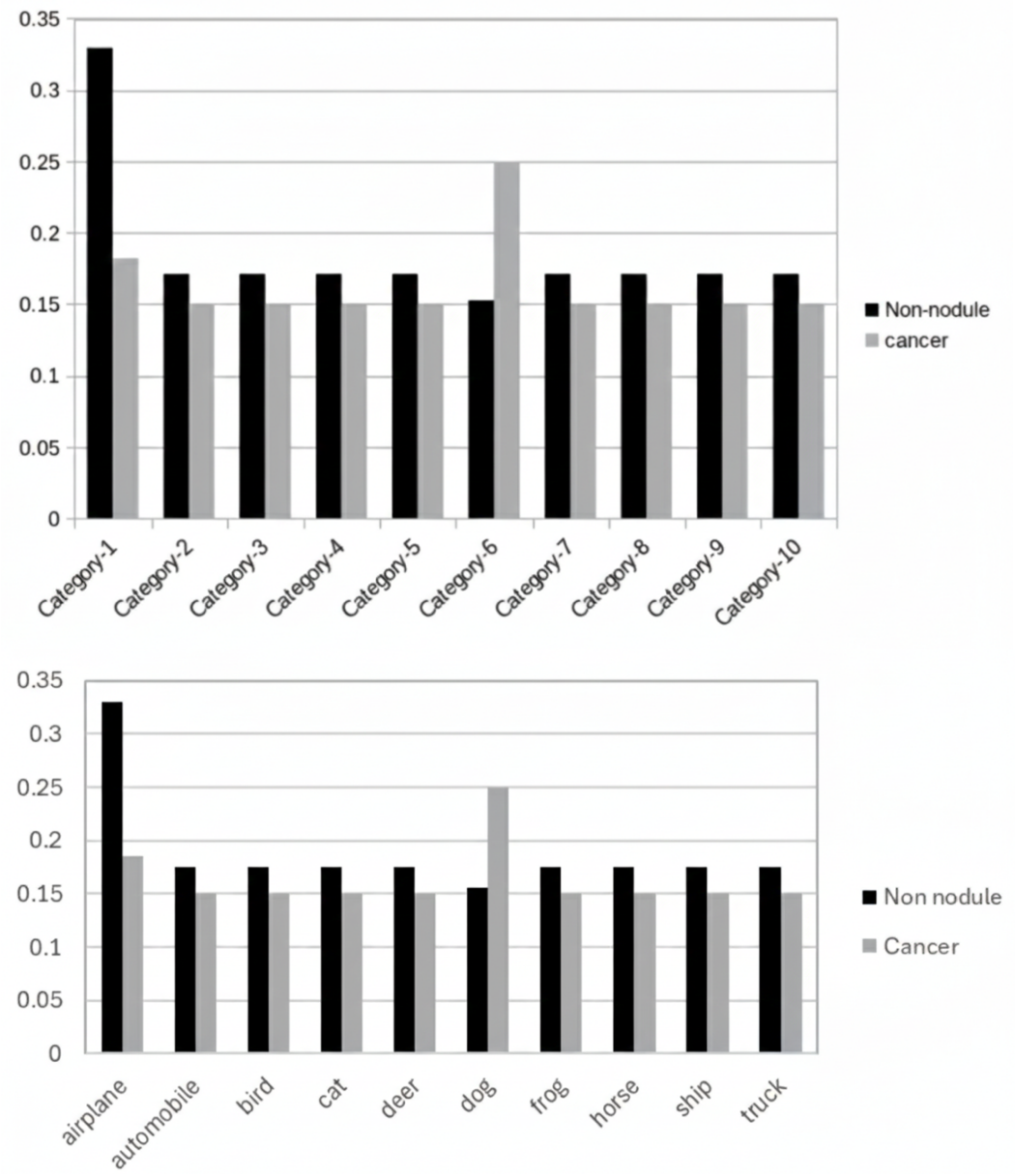

Figure 4. Correlation between cifar-10 and JSRT dataset

Table 1. Performance for different couple source-target dataset

	Performance
JSRT without transfer learning	65.4%
MNIST case 1 (digit 0, digit 8)	73.2%
MNIST case 2 (digit 6, digit 0)	75.5%
cifar10 (airplane, dog)	87.2%

Table 2. Performance for variation step of mean field

	Performance
Non-Mean Field	75.4%
1-step Mean Field	78.6%
5-step Mean Field	87.2%
10=step Mean Field	89.4%

Table 1. shows the results of the performance for different couple source-target dataset. Overall, transfer learning gives better performance than DBM with a small number of x-ray dataset.These results indicate that high correlation between source and target data provides better performance. The results confirms that transfer learning improves performance compared to DBM without transfer (65.4%). The higher accuracy obtained from CIFAR-10 (87.2%) compared to MNIST (73-75%) is consistent with the stronger correlations shown in Figure 4. This suggests that structural and textural similarity between the source and target images plays a critical role in enabling transferability. Categories such as airplane and dog exhibit edge contrasts and texture patterns more consistent with lung X-rays, which may explain their superior contribution to classification accuracy (Ranzato et al., 2010; Ait Nasser et al., 2023). Table 2. shows the results of the performance for variation step number of mean field for cifar10 (airplane, dog) case. This result shows a greater number of mean-field iterations giving improve the performance. However, a large number of iterations lead to slower calculation times. The results shows that increasing the number of mean-field iterations improves performance, with accuracy peaking at 89.4% using 10 steps. This demonstrates that deeper inference provides more accurate representations for classification. However, it also increases computational cost. In this study we did not record exact computation times, but we acknowledge this limitation and will include detailed profiling of training efficiency in future work.

These findings demonstrate that TL-DBM is effective for lung cancer classification even with small datasets, achieving accuracy up to 89.4%. The main strength of DBMs lies in their generative modeling capabilities, which allow them to transfer hierarchical representations across domains (Salakhutdinov & Larochelle, 2010; Srivastava & Salakhutdinov, 2012). This makes them suitable for medical imaging contexts where labeled data are scarce. However, DBMs require more intensive computation, careful parameter tuning, and longer training times compared to CNN-based transfer learning (Bengio, 2009; Ranzato et al., 2010). Moreover, CNNs and, more recently, transformer models dominate current medical imaging practice (Litjens et al., 2017; Shen et al., 2017), while DBMs are less widely adopted. Nevertheless, our results show that TL-DBM remains a viable approach under limited-data conditions and should be further evaluated in comparison with CNN and transformer-based methods using larger datasets.

Conclusions

This study demonstrates the effectiveness of classifying lung cancer using a deep learning framework that combines Transfer Learning with Deep Boltzmann Machines (TL-DBM), particularly in scenarios with limited chest X-ray data. By standardizing image formats and sizes through preprocessing, we enabled the DBM to be pretrained on large-scale datasets such as MNIST and CIFAR-10. The pretrained parameters were then transferred to train on the smaller, domain-specific dataset.

We introduced a correlation-based method to select source data categories that align closely with

the target medical images. Additionally, we examined the role of mean-field iterations in improving classification performance during the DBM fine-tuning process. Among the tested configurations, using the CIFAR-10 dataset—specifically the airplane and dog categories—as source data, along with a 10-step mean-field update, achieved the highest accuracy of 89.4%.

These findings suggest that TL-DBM offers a viable solution for applying deep learning in medical imaging tasks where labeled data is scarce. The model's adaptability also opens pathways for future research using richer datasets such as ImageNet, which could further enhance generalization across various clinical imaging tasks.

Conflicts of Interest

The authors declare that there is no conflict of interest regarding the publication of this paper.

Acknowledgment

This research is funded by Penelitian, Pengabdian Masyarakat dan Inovasi (PPMI) ITB 2022.

References

Ait Nasser, I., Mahfoudhi, E., Trabelsi, D., & Bouhlel, M. S. (2023). Deep learning for pneumonia detection from chest X-ray images: A comprehensive review. *Medical Image Analysis*, 87, 102825.

Bengio, Y. (2009). Learning deep architectures for AI. *Foundations and Trends in Machine Learning*, 2(1), 1–127.

Bengio, Y., Lamblin, P., Popovici, P., & Larochelle, H. (2007). Greedy layer-wise training of deep networks. In *Advances in Neural Information Processing Systems* (Vol. 19). MIT Press.

Deng, L. (2012). The MNIST database of handwritten digit images for machine learning research. *IEEE Signal Processing Magazine*, 29(6), 141–142.

Eertink, J. J., Dagnelie, P. C., van der Velden, J. M., Zwezerijnen, B. G., et al. (2022). External validation: A simulation study to compare cross-validation, hold-out validation, and small test sets. *Journal of Evaluation in Clinical Practice*, 28(5), 1031–1041.

Hinton, G. E., Osindero, S., & Teh, Y. W. (2006). A fast learning algorithm for deep belief nets. *Neural Computation*, 18, 1527–1554.

Hussain, L., Nguyen, T., Li, H., Abbasi, A. A., Lone, K. J., Zhao, Z., & Chen, M. (2020). A rapid AI-based COVID-19 diagnostic system using chest X-ray images. *BioMedical Engineering OnLine*, 19, 1–12.

Jensen, A. R., Mainz, J., & Overgaard, J. (2002). Impact of delay on diagnosis and treatment of primary lung cancer. *Acta Oncologica*, 41(2), 147–152.

Krizhevsky, A., Nair, V., & Hinton, G. (n.d.). CIFAR-10 dataset. https://www.cs.toronto.edu/~kriz/cifar.html

Litjens, G., Kooi, T., Bejnordi, B. E., Setio, A. A. A., Ciompi, F., Ghafoorian, M., van der Laak, J. A. W. M., van Ginneken, B., & Sánchez, C. I. (2017). A survey on deep learning in medical image analysis. *Medical Image Analysis*, 42, 60–88.

Najafabadi, M. M., Villanustre, F., Khoshgoftaar, T. M., Seliya, N., Wald, R., & Muharemagic, E. (2015). Deep learning applications and challenges in big data analytics. *Journal of Big Data*, 2(1), 1–21.

Pan, S. J., & Yang, Q. (2010). A survey on transfer learning. *IEEE Transactions on Knowledge and Data Engineering*, 22(10), 1345–1359.

Raghu, M., Zhang, C., Kleinberg, J., & Bengio, S. (2019). Transfusion: Understanding transfer learning for medical imaging. In *Advances in Neural Information Processing Systems* (Vol. 32).

Ranzato, M., Krizhevsky, A., & Hinton, G. (2010). Factored 3-way restricted Boltzmann machines for modeling natural images. In *Proceedings of the Thirteenth International Conference on Artificial Intelligence and Statistics (AISTATS)* (pp. 621–628).

Salakhutdinov, R., & Larochelle, H. (2010). Efficient learning of deep Boltzmann machines. In *Proceedings of the Thirteenth International Conference on Artificial Intelligence and Statistics (AISTATS)* (pp. 693–700). JMLR Workshop and Conference Proceedings.

Shen, D., Wu, G., & Suk, H. I. (2017). Deep learning in medical image analysis. *Annual Review of Biomedical Engineering*, 19, 221–248.

Shiraishi, J., Katsuragawa, S., Ikezoe, J., et al. (2000). Development of a digital image database for chest radiographs with and without a lung nodule: Receiver operating characteristic analysis of radiologists' detection of pulmonary nodules. *AJR American Journal of Roentgenology*, 174, 71–74.

Srivastava, N., & Salakhutdinov, R. (2012). Multimodal learning with deep Boltzmann machines. In *Advances in Neural Information Processing Systems* (Vol. 25, pp. 2222–2230).

Sung, H., Ferlay, J., Siegel, R. L., Laversanne, M., Soerjomataram, I., Jemal, A., & Bray, F. (2021). Global cancer statistics 2020: GLOBOCAN estimates of incidence and mortality worldwide for 36 cancers in 185 countries. CA: *A Cancer Journal for Clinicians*, 71(3), 209–249.

Torrey, L., & Shavlik, J. (2010). Transfer learning. In *Handbook of research on machine learning applications and trends: Algorithms, methods, and techniques* (pp. 242–264). IGI Global.

Willemink, M. J., Koszek, W. A., Hardell, C., Wu, J., Fleischmann, D., Harvey, H., … Lungren, M. P. (2020). Preparing medical imaging data for machine learning. *Radiology*, 295(1), 4–15.